

Scientific paper

# Investigation of Biological and Prooxidant Activity of Zinc Oxide Nanoclusters and Nanoparticles

Iliana A. Ivanova,<sup>1</sup> Elitsa L. Pavlova,<sup>2</sup> Aneliya S. Kostadinova,<sup>3</sup>  
Radostina D. Toshkovska,<sup>1,4</sup> Lyubomira D. Yocheva,<sup>5</sup> Kh El-Sayed,<sup>6,7</sup>  
Mohamed A. Hassan,<sup>6,7</sup> Heba El-Sayed El-Zorkany<sup>6,7</sup> and Hisham A. Elshoky<sup>6,7,8\*</sup>

<sup>1</sup> Dept. Microbiology, Faculty of Biology, Sofia University Saint Kliment Ohridski, 8 Dragan Tsankov Blvd, 1164 Sofia, Bulgaria

<sup>2</sup> Faculty of Physics, Sofia University “St. Kliment Ohridski”, 5 James Bourchier Blvd., 1164 Sofia, Bulgaria

<sup>3</sup> Institute of biophysics and biomedical engineering, Bulgarian academy of science, Akad. Georgi Bonchev 21str, Sofia 1113, Bulgaria

<sup>4</sup> Institute of Organic Chemistry with Center of Phytochemistry, 9 Acad. G. Bonchev Str, Sofia

<sup>5</sup> Faculty of Medicine, 1 Kozyak Str, 1407, Sofia, Bulgaria

<sup>6</sup> Nanotechnology and Advanced Materials Central Lab, Agricultural Research Center, Giza, Egypt

<sup>7</sup> Regional Center for Food and Feed, Agricultural Research Center, Giza, Egypt.

<sup>8</sup> Tumor Biology Research Program, Department of Research, Children’s Cancer Hospital Egypt 57357, P.O Box 11441, 1 Seket Al-Emam Street, Cairo, Egypt

\* Corresponding author: E-mail: heshamalshoky@sci.cu.edu.eg; heshamalshoky@gmail.com

Received: 12-13-2021

## Abstract

Zinc oxide (ZnO) nanomaterials offer some promising antibacterial effects. In this study, a new form of ZnO is synthesized, named ZnO nanocluster bars (NCs). Herein, ZnO NCs, ZnO nanoparticles (NPs), ZnO coated with silica (ZnO-SiO<sub>A</sub>, ZnO-SiO<sub>B</sub>), and SiO<sub>2</sub> NPs were prepared, characterized, and their antimicrobial and prooxidant activity were tested. The prooxidant activity of all nanomaterials was studied according to free-radical oxidation reactions (pH 7.4 and pH 8.5) in chemiluminescent model systems. Each form of new synthesized ZnO nanomaterials exhibited a unique behavior that varied from mild to strong prooxidant properties in the Fenton’s system. ZnO NPs and ZnO NCs showed strong antibacterial effects, ZnO-SiO<sub>A</sub> NPs did not show any antibacterial activity representing biocompatibility. All tested NMs also underwent oxidation by H<sub>2</sub>O<sub>2</sub>. ZnO NCs and ZnO NPs exhibited strong oxidation at pH 8.5 in the O<sub>2</sub><sup>-</sup> generating system. While, SiO<sub>2</sub>, ZnO-SiO<sub>A</sub> and ZnO-SiO<sub>B</sub> possessed pronounced 60–80% antioxidant effects, SiO<sub>2</sub> NPs acted as a definitive prooxidant which was not observed in other tests. ZnO NCs are strongly oxidized, assuming that ZnO NCs provide a slower release of ZnO, which leads to having a stronger effect on bacterial strains. Thus, ZnO NCs are an important antibacterial agent that could be an emergent replacement of traditional antibiotics.

**Keywords:** ZnO; nanoclusters; nanocomposites; antimicrobial activity; ROS; chemiluminescence.

## 1. Introduction

Multi-drug resistant (MDR) bacteria have become an important problem because of the extensive use of antibiotics, which are often applied without proper medical indications. The inappropriate selection and switch between antimicrobial alternates cause “selection pressure.” All

of this causes MDR bacteria. Consequently, while many studies have focused on identifying new effective bactericidal materials, new alternative strategies for combating bacterial resistance remain under investigation.<sup>1–4</sup>

Nanotechnology introduces a special solution to the MDR bacteria. Several nanomaterials (NMs) have been used in antibacterial treatments, antibacterial vaccines,

antibiotic delivery carriers, and antibacterial coatings for implantable devices and medicinal materials to prevent infection and promote infection wound healing to help control bacterial infections. They are applied in microbial diagnostic systems too.<sup>5</sup>

ZnO is known for its anti-inflammatory, astringent, and soothing effects.<sup>6,7</sup> Therefore, ZnO has been used in cosmetics, including sunscreens, toothpaste, and shampoos, after the nineteenth century.<sup>8</sup> Furthermore, the US Food and Drug Administration (FDA) has classified ZnO as “Generally Recognized as Safe” (GRAS) because of its non-toxic properties. Zn is used as a food additive too.<sup>9,10</sup> Recently, ZnO NMs have attracted considerable attention because of their antimicrobial activity. ZnO NMs’ superiority in fighting microbial resistance is attributed to their nonspecific activity, small particle size, high surface area, low cost, and efficiency against various bacteria with low toxicity to human cells.<sup>11</sup>

Unfortunately, we have limited knowledge of NMs’ mechanisms of action against bacteria. The suggested mechanisms include oxidative stress induction, metal ion release, and non-oxidative mechanisms.<sup>5,12,13</sup> The bacterial destruction by ZnO NMs is believed to follow two pathways: binding to cell membranes, consequently disrupting their potential and integrity and inducing generation of reactive oxygen species (ROS).<sup>5</sup> ZnO NMs are mutagens albeit weak ones.<sup>14</sup>

Many studies attempted to investigate and use ZnO nanoparticles in different applications.<sup>15,16</sup> Smaller ZnO nanoparticles usually show higher cellular inhibition activity. Furthermore, surface modification of ZnO NMs can affect their properties that may change or improve their antimicrobial activity.<sup>17</sup>

While the generation of ROS is important for antibacterial activity of ZnO NMs, it is necessary to investigate the kinetics of free radical generation, affected by ZnO NMs.<sup>18,19</sup> The chemiluminescent assay is a convenient method for such studies. It can be used to monitor the dynamics of free radical reactions and to determine their prooxidant/antioxidant activity. The chemiluminescent technique is advantageous because of its accuracy, sensitivity, high speed, and relatively low cost; moreover, it requires a small sample volume. Many physical and chemical probes, such as luminol and lucigenin, can be used to enhance chemiluminescence. These reactions are accompanied by emission in the range of 480–580 nm; hence, they can be harnessed to assess the quantum yield of generated free radicals.<sup>20–22</sup>

We synthesized a completely new form of ZnO nanoaggregates in this study called ZnO nanocluster bars (ZnO NCs). Their prooxidant and antimicrobial effects were evaluated compared with different forms of ZnO NMs as spherical ZnO NPs with/without silica coating. Furthermore, the prooxidant activity of all NMs was examined as free radical oxidation reactions at pH 7.4 and pH 8.5 in chemiluminescent model systems.

## 2. Experimental

### 2. 1. Materials

The materials used in this study were purchased with high purity; zinc acetate dihydrate (99.5%, Merck, Germany), 2-propanol (99.9%, Sigma-Aldrich), sodium hydroxide (99.5%, Sigma-Aldrich), tetraethyl orthosilicate (TEOS, 98%, Sigma-Aldrich), iron sulphate (P. A.) (Merck, Germany), ammonia solution (25%, Sigma-Aldrich), phenazine methosulfate (PhMS) (N-methylidibenzopyrazine methyl sulfate salt) (P. A.) (Merck, Germany), hydrogen peroxide (30%) (Boron, Bulgaria), disodium hydrogen phosphate (P. A.) (Boron, Bulgaria), citric acid (P. A.) (Boron, Bulgaria), lucigenin (bis-N-methylacridinium nitrate) (P. A.) (Aldrich, USA),  $\beta$ -nicotinamide adenine dinucleotide, reduced form (P. A.) (NAD.H, Boehringer, Germany) and dimethyl sulfoxide (P. A.) (DMSO, Aldrich, USA). All chemicals were used as-purchased without further purification.

### 2. 2. Preparation of ZnO Nanocluster Bars (ZnO NCs)

A solvothermal process prepared the ZnO nanocluster bars as follows; 1 g of zinc acetate was ultrasonically dispersed in 80 mL of 2-propanol in a 150 mL beaker for 30 min at room temperature. Then, 2 g of oxalic acid was added followed by another 30 min of ultrasonication. To complete the hydrothermal preparation process, the mixture was poured from the beaker in a Teflon-based stainless steel autoclave and placed in the oven for 24 h at 180 °C. Subsequently, the prepared NPs were washed three times with DI-H<sub>2</sub>O and ethanol by centrifugation (4500 rpm at 10 °C for 30 min.), the same step was repeated for DI-H<sub>2</sub>O and ethanol three times until the whole quantity is washed. The precipitate was dried in an oven at 180 °C for 8 h. Then, the powder was calcined in a muffle oven at 400 °C for 2 h.

### 2. 3. Preparation of ZnO Nanoparticles (ZnO NPs)

ZnO nanoparticles were obtained using a modified method as described by G. Simonelli et. al.<sup>23–25</sup> Briefly, a 46.5 mM of zinc acetate dihydrate was prepared by dissolving 2.195 g in 20 mL of 2-propanol at 50 °C and then the volume was increased to 210 mL by 2-propanol. Note that 0.8 g of sodium hydroxide in 40 mL solution (35 mL 2-propanol + 5 mL DI-H<sub>2</sub>O) was added under continuous stirring in an ice bath. Then, the solution was stirred at 60 °C for 2 h, and the temperature was measured and followed up to ensure that it did not rise over that because this influenced the particle sizes. Subsequently, the preparation vessel was kept stable at room temperature for three days for additional aging. Then, the sample was repeatedly centrifuged at

7000 rpm/15 min till all other chemical residuals were completely removed. The precipitate was dried in the oven at 180 °C for 8 h. Then, the powder was calcined in a muffle oven at 400 °C for 2 h. Characterization measurements were performed using DLS, zeta potential, XRD and TEM.

## 2. 4. Preparation of Silica Capped ZnO NPs (ZnO-SiO<sub>A,B</sub>)

ZnO NPs were dispersed in water as per Bartczak's protocol with modification.<sup>18,26</sup> In an ultrasonic bath, 0.5 g of ZnO NPs in 100 mL of 2-propanol was sonicated for 15 min at room temperature. The pH of the ZnO NP solution was increased to 10 by the dropwise addition of 1 M ammonium hydroxide solution and monitoring the change using a pH meter. Next, 100 mL of 2% TEOS in DI-H<sub>2</sub>O was added, and the suspension was sonicated for 1 h at room temperature. NPs then reacted overnight at 60 °C with stirring before purification from excess by-products and organic solvent residues by triple centrifugation (13000 rpm, 15 min at room temperature) with the same approach mentioned for ZnO NC preparation. (ZnO-SiO<sub>A</sub>) NPs were then dried in a hot air oven at 80 °C overnight. For the second form of SiO<sub>2</sub> capped ZnO NPs (ZnO-SiO<sub>B</sub>), the same procedure was performed but without pH adjustment of the ZnO solution.

## 2. 5. Preparation of Silica Nanoparticles (SiO<sub>2</sub> NPs)

In brief, 300 mL of DI-H<sub>2</sub>O was added to 300 mL ethanol and stirred for 10 min at room temperature. Then, 45 mL of TEOS were added and sonicated for 20 min. The dropwise additions of 1 M ammonium hydroxide solution were made until pH 10 was reached, and the reaction was stirred overnight. Next, the SiO<sub>2</sub> NPs were washed well with DI-H<sub>2</sub>O using centrifugation at 10000 rpm for 15 min, using the same procedure as before, until ammonia odor disappears and pH becomes neutral. The precipitate was dried in the oven at 45 °C overnight; finally, the yield was ground to obtain a fine silica powder.<sup>26</sup>

## 2. 6. Characterization of the Prepared Nanoparticles

A transmission electron microscope (TEM, Tecnai G20, FEI, Netherlands) was used for imaging the nano-materials that were prepared. The bright field imaging was employed at an accelerating voltage of 200 kV using a lanthanum hexaboride (LaB<sub>6</sub>) electron source gun, and the Eagle CCD camera was used to acquire and collect transmitted electron images with an image resolution (4K x 4K). Before imaging, the aqueous suspensions of prepared nanoparticles were prepared in an ultrasonicator (SB-120DTN, Taiwan) for 10 min, and then particles were

deposited from a dilute aqueous suspension onto a 200 mesh-carbon coated copper grid placed on filter paper and left for drying at room temperature as a common method for preparing TEM samples.

However, powder X-ray diffraction (XRD – X'Pert PRO, PANalytical, The Netherlands) was used to reveal the crystal structure of the prepared NMs. XRD operated at 45 kV and 30 mA using X-ray source “Cu K $\alpha$  radiation” ( $\lambda = 1.5404 \text{ \AA}$ ). The step time and step sizes were 0.5 s/step and 0.02 degree/step, respectively, in the range of 4° – 80° (2 $\theta$ ). Peaks matching and analysis were performed using high score plus software.

Particle size distribution analysis and zeta potentials of the prepared materials were measured using Zetasizer Nano S, Malvern Instruments, UK, to evaluate hydrodynamic size and surface charge. These measurements were performed in aqueous solutions after NMs were dispersed in deionized water using an ultrasonicator for 15 minutes to obtain stable suspensions. A portion of suspension was transferred in 10 mm x 10 mm cuvette (DTS1070) to measure particle size and zeta potential.

## 2. 7. Microorganisms

The antimicrobial activity was tested against Gram-positive *Bacillus cereus* NBIMCC1095, *Staphylococcus epidermidis* ATCC 12228 bacteria, and Gram-negative *Escherichia coli* BL21DE3 bacteria. All bacteria purchased from National Bank for Industrial Microorganisms and Cell Cultures (NBIMCC, Bulgaria) were grown in nutrient broth (NB Conda, Spain) at 37 °C and 180 rpm (shaker Rotomax, incubator ED053, Germany) for 24 h with two sub-cultivations. Microbial density of cultures in an exponential phase of 0.5–0.6 was determined according to McFarland.

## 2. 8. Antimicrobial Activity

Antibacterial influence of each type of prepared NMs was investigated using spot-diffusion in agar. Briefly, 100  $\mu$ L of each bacterial suspension was homogeneously spread on nutrient agar plates. 10  $\mu$ L drops of investigated material were put on inoculated solid medium. Plates were left for 2 h at 4–6 °C to afford diffusion of dispersions and cultured for 24 h, and then 48 h at 37 °C. The diameters of sterile zones were measured in mm.<sup>27,28</sup>

## 2. 9. Chemiluminescent Assay

The chemiluminescent method was applied to study effect of NMs on the kinetics of free-radical oxidation reactions using activated chemiluminescence and the probe lucigenin.<sup>29</sup>

The higher acidity of medium favors radical formation reactions and enables the achievement of reliable differences. Two different pH systems were investigated –

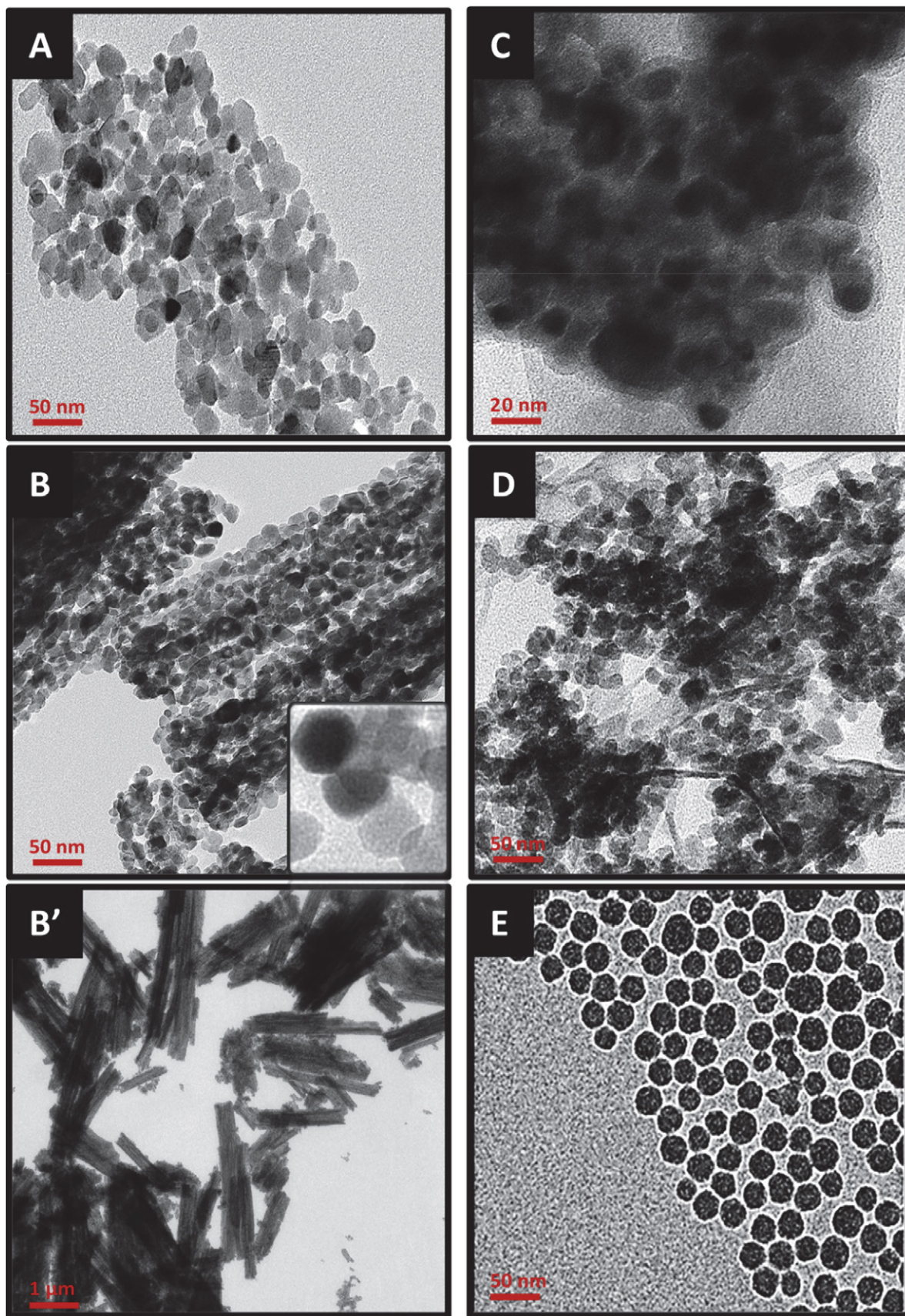


**Figure 1:** TEM images of (A) ZnO-NPs, (B and B') different magnifications of ZnO nanocluster bars, (C) ZnO-SiO<sub>A</sub>, (D) ZnO-SiO<sub>B</sub>, and (E) SiO<sub>2</sub> NPs, respectively.

pH 7.4 and pH 8.5, physiological and alkaline. Three *ex vivo* model systems were implemented in buffers and here described briefly.<sup>22</sup> First system, generating hydroxyl radicals ( $\cdot\text{OH}$ ) system, it contains 0.2 mol of sodium hydrogen phosphate buffer, with the appropriate pH, Fenton's reagent [ $\text{FeSO}_4$  ( $5 \cdot 10^{-4}$  mol) –  $\text{H}_2\text{O}_2$  (1.5%), lucigenin ( $10^{-4}$  mol)] and NMs.

The second system contains the oxidant hydrogen peroxide ( $\text{H}_2\text{O}_2$ ): 0.2 mol sodium hydrogen phosphate buffer, with appropriate pH,  $\text{H}_2\text{O}_2$  (1.5%), the chemiluminescent probe lucigenin ( $10^{-4}$  mol), and NMs. The third system is for the generation of superoxide radicals ( $\text{O}_2^{\cdot-}$ ) through the reaction NAD.H-PhMS. It contains 0.2 mol of sodium hydrogen phosphate buffer with the specific pH, NAD.H ( $10^{-4}$  mol), phenazine-metasulfate ( $10^{-6}$  mol), lucigenin ( $10^{-4}$  mol) and NMs. The control samples do not contain any NMs. The reactions are monitored for 3 minutes every 3 seconds; the maximum peak for each curve was obtained.

## 2. 10. Statistics

All experiments were performed in triple reproducible measurements; statistical analysis was implemented using Origin 8.5 and Microsoft Office Excel 2010. To measure the strength of the relationship between tested variables, correlation coefficients ( $r$ ) between the sensitivity of the selected bacterial strains toward the antimicrobial effect of ZnO NPs, ZnO NCs, ZnO- $\text{SiO}_A$ , and ZnO- $\text{SiO}_B$  NMs tested by spot diffusion and chemiluminescent assays are calculated.

## 3. Results and Discussion

### 3. 1. Characterization

#### Transmission electron microscopy (TEM) imaging

Fig. 1 shows the TEM micrographs of ZnO NMs and  $\text{SiO}_2$  NPs. TEM images (Fig. 1A, B, and B') demonstrated that ZnO NPs and ZnO NCs agglomerated to certain extent. The average diameter size, measured using TEM-TIA software, of the prepared ZnO-NPs (Fig. 1A, B) and  $\text{SiO}_2$  NPs (Fig. 1E) was between 22.9–38.1 and 19–25 nm. The ZnO NCs agglomerated in NCs with a length of 2–3  $\mu\text{m}$  and a width between 200 and 350 nm. The image of ZnO NCs comprised small ZnO NPs with an average particle size of 14.3–21.5 nm. However, ZnO- $\text{SiO}_2$  NPs demonstrated two different morphological forms. Fig. 1C shows a homogeneous sphere capped ZnO- $\text{SiO}_A$  NPs with an average diameter of  $\sim 20 \pm 3$  nm, and the silica layer surrounding the ZnO NPs with an estimated layer thickness of  $4 \pm 0.5$  nm. However, ZnO- $\text{SiO}_B$  show in Fig. 1D with less homogeneity in particle size and additional aggregation than ZnO- $\text{SiO}_A$  with an average particle size of  $13.4 \pm 3$  nm for ZnO cores and  $3.5 \pm 0.7$  nm for  $\text{SiO}_2$  cap. Fig. 1E shows well-dispersed and homogeneous spherical  $\text{SiO}_2$  NPs with an average  $38 \pm 3$  nm diameter. The change in the shape depends on the method of preparation, which causes the  $\text{SiO}_2$  NPs to appear to be in a good and homogeneous shape.

#### X-ray diffraction (XRD) analysis

Fig. 2(a–e) shows the XRD patterns for ZnO NPs-, ZnO NCs-, and  $\text{SiO}_2$ -coated ZnO and  $\text{SiO}_2$ . All the dif-

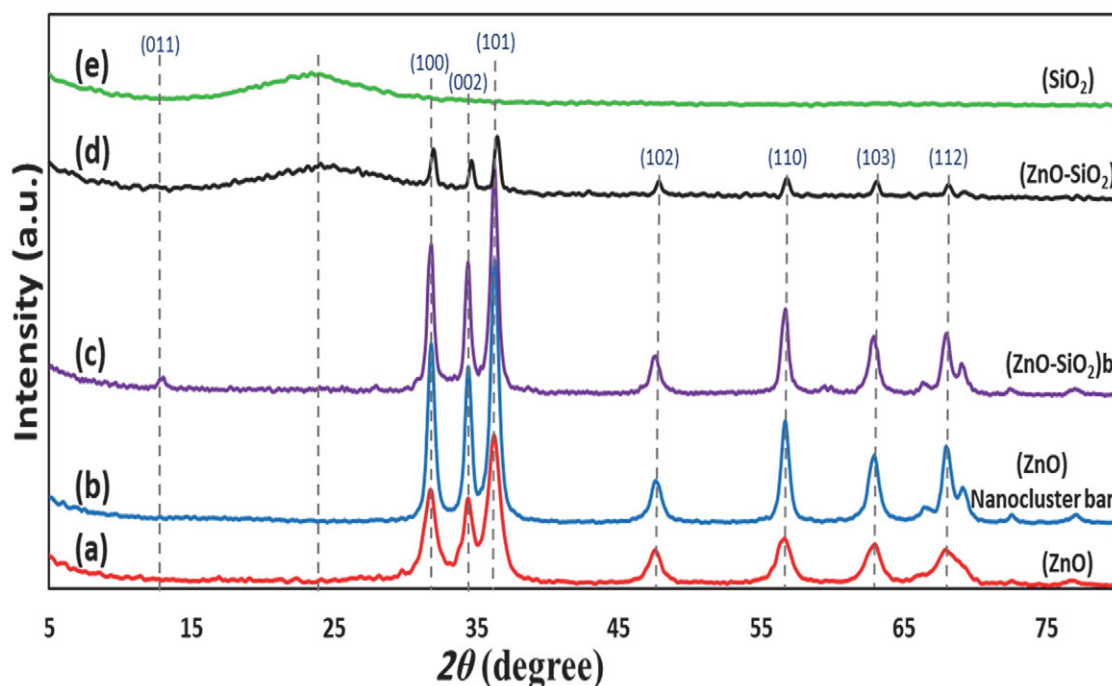


Figure 2: XRD patterns of (a) ZnO NPs, (b) ZnO NC bars, (c) ZnO- $\text{SiO}_{2A}$ , (d) ZnO- $\text{SiO}_{2B}$ , and (e)  $\text{SiO}_2$  NPs, respectively.

fraction peaks of ZnO-containing materials are fitted to the hexagonal (wurtzite) ZnO structure (JCPDS no. 01–080–3002) with lattice parameters ( $a = b = 3.25$  Å,  $c = 5.21$  Å), and a space group  $P63$  mc. The primary peaks of ZnO appeared at diffraction angles of  $2\theta$ : 31.8°, 34.4°, 36.2°, 47.5°, 56.6°, 62.8°, and 67.9° for ZnO NPs and ZnO NCs. While the SiO<sub>2</sub>-coated ZnO NPs present a combination of SiO<sub>2</sub> peaks at  $2\theta = 23.2^\circ$  and ZnO diffraction peaks with a slight peak shifting (Fig. 2c). This may indicate a complete formation of SiO<sub>2</sub>-coated ZnO nanostructure. Furthermore, Figure 2d shows the diffraction peaks of pure SiO<sub>2</sub> with a broad distinguished peak at 23.2°, which is well-matched with the JCPDS card (no. 01–077–9207). All XRD patterns show highly pure materials with no contamination.

### Particles size distribution analysis and zeta-potential measurements

Table 1 shows the particle size distributions and zeta potential measurements for ZnO NPs, ZnO NCs, SiO<sub>2</sub>-coated ZnO (A&B), and SiO<sub>2</sub> NPs. The average hydrodynamic diameter of ZnO, SiO<sub>2</sub>-coated ZnO (A&B), and SiO<sub>2</sub> NPs is  $46.0 \pm 4.9$ ,  $49.3 \pm 8.4$ ,  $48.5 \pm 6.7$ , and  $68.7 \pm 9.4$  nm, respectively, which demonstrates a homogeneous size distribution. Increasing hydrodynamic diameters for SiO<sub>2</sub>-coated ZnO (A&B) rather than ZnO NPs appear from the shell layer of SiO<sub>2</sub> on the core particles of ZnO. However, the results shown from ZnO NCs are  $1968 \pm 237$  nm because of intensive agglomerations of ZnO nanoparticles suspended in an aqueous solution. However, the zeta potential measurements show a negative charge on the prepared NMs except SiO<sub>2</sub>-coated ZnO (B), which was prepared without adjusting the pH. The pH of the preparation medium plays an important role in the surface charge and zeta potential results. As the pH increased, the surface tendency of the prepared materials to carry more negative charges increased.

The antimicrobial activity

### The antimicrobial activity

The antimicrobial effect of NMs was determined using the spot diffusion test. Most of the nanoparticles possess a contact killing effect that could not be demonstrated.

**Table 1:** The particles size distributions and zeta potential measurements of ZnO NPs, ZnO NCs, and SiO<sub>2</sub>-coated ZnO (A&B) and SiO<sub>2</sub>

	ZnO	ZnO cluster	ZnO-SiO <sub>A</sub>	ZnO-SiO <sub>B</sub>	SiO <sub>2</sub>
<b>Particle size diameter (nm)</b>	$46.0 \pm 4.9$	$1968 \pm 237$	$49.3 \pm 8.4$	$48.5 \pm 6.7$	$68.7 \pm 9.4$
<b>Zeta-Potential (mV)</b>	$-16.5 \pm 5.4$	$-11.37 \pm 2.7$	$-21.78 \pm 6.3$	$19.3 \pm 4.2$	$-27.2$

**Table 2.** Inhibition zones (mm) of the tested bacteria

Nanoparticles	Nanoparticles Concentration (mg/mL)	Tested microorganisms* Inhibition zones (mm)		
		<i>E. coli</i> (BL21DE)	<i>B. cereus</i> (NBIMCC1095)	<i>S. epidermidis</i> (ATCC 12228)
ZnO NPs	3	$10 \pm 0.5$	$6 \pm 0.5$	$13 \pm 0.5$
	1.5	$10 \pm 0.5$	0	$10 \pm 0.5$
	0.5	0	0	0
	0.25	0	0	0
ZnO NCs	3	$10 \pm 0.5$	$9.5 \pm 0.5$	$15 \pm 0.5$
	1.5	0	$8 \pm 0.5$	$8 \pm 0.5$
	0.5	0	$5 \pm 0.5$	0
	0.25	0	$4 \pm 0.5$	0
ZnO-SiO <sub>A</sub>	3	0	0	0
	1.5	0	0	0
	0.5	0	0	0
	0.25	0	0	0
ZnO-SiO <sub>B</sub>	3	$10 \pm 0.5$	$10 \pm 0.5$	$15 \pm 0.5$
	1.5	0	$8 \pm 0.5$	$7 \pm 0.5$
	0.5	0	0	0
	0.25	0	0	0
SiO <sub>2</sub>	3	0	0	0
	1.5	0	0	0
	0.5	0	0	0
	0.25	0	0	0

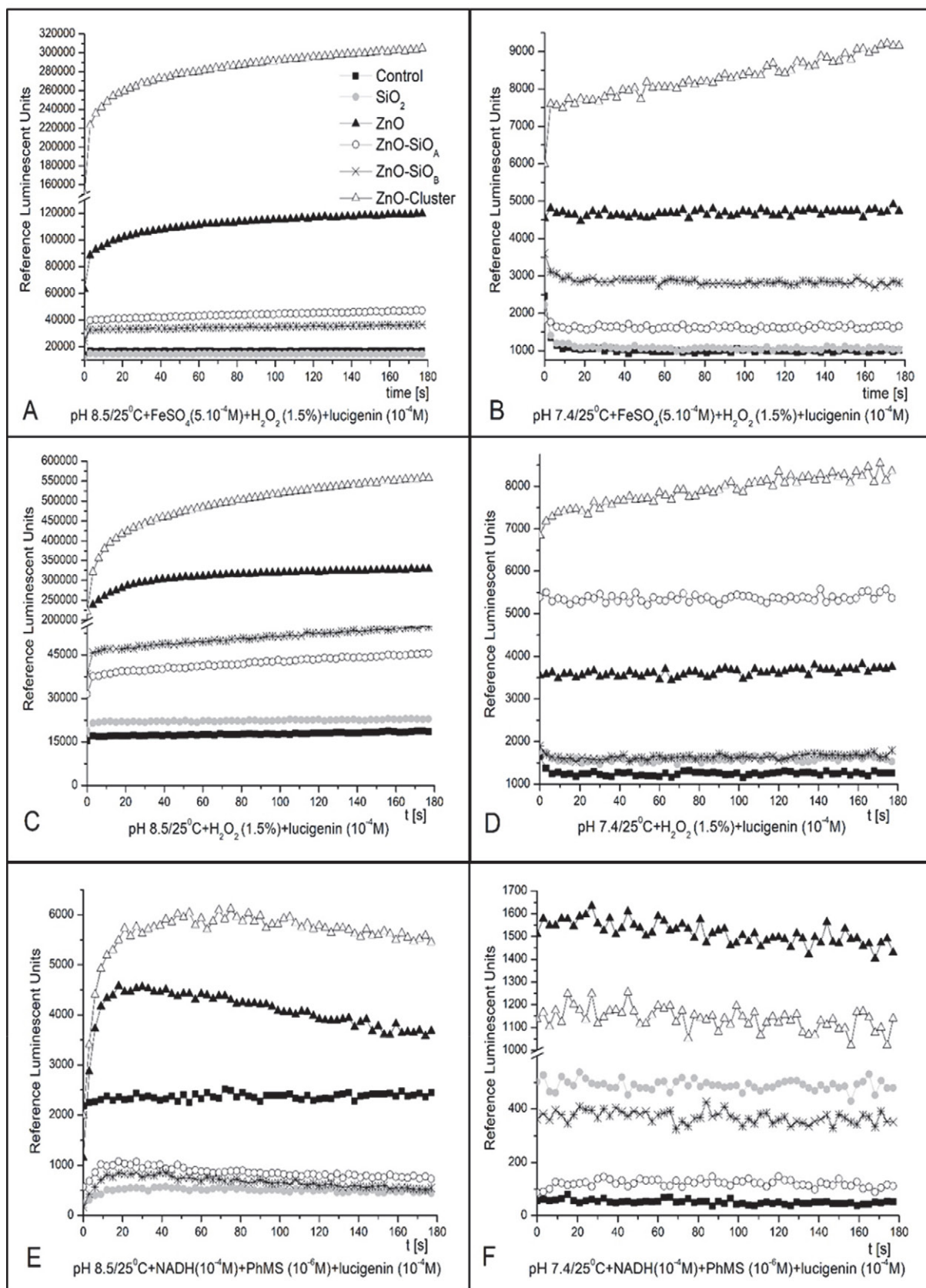


**Figure 3.** Chemiluminescence induced in the Fenton's system (system I: A, B), by H<sub>2</sub>O<sub>2</sub> (system II: C, D) and O<sub>2</sub><sup>-</sup> radicals (system III: E, F) in seconds, at pH 8.5 and 7.4 in the presence/absence of NMs.

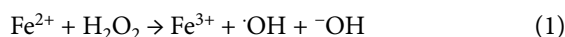
ed if nanomaterials are dropped on paper disks or in agar wells, because of impossible agar diffusion or diminishing of the nanoparticle–bacteria interaction.<sup>27</sup>

From the results, it is obvious that the SiO<sub>2</sub> NPs and ZnO-SiO<sub>A</sub> were completely safe at concentrations up to 3 mg/mL; however, all other tested materials showed bactericidal effects at a higher concentration than 3 mg/mL. All tested bacteria show high sensitivity against ZnO NPs at 3 mg/mL, while only *E. coli* and *S. epidermidis* were inhibited at 1.5 mg/mL. While, lower concentrations of ZnO NPs were safe on all the tested bacteria. Furthermore, ZnO-SiO<sub>A</sub> was completely safe on bacteria at all concentrations; however, ZnO-SiO<sub>B</sub> showed higher toxicity compared to the naked silica particles. ZnO NCs have shown the largest sterile zones at the diffusion test and demonstrated the strongest antibacterial effect if used in concentrations of 3 mg/mL or less. As shown in Table 2, the most sensitive of all three tested bacteria were *Bacillus cereus* compared to *E. coli* and *S. epidermidis*.

ZnO NMs, and many metal oxide nanoparticles, possess bactericidal properties because of the generation of ROS. The chemiluminescent method was used to trace the concentration and kinetics of ROS generation by determining the quantum yields of these reactions in the 480–580 nm range. Three chemiluminescent model systems were applied.

#### • System I

The interaction between Fe<sup>2+</sup> ions and H<sub>2</sub>O<sub>2</sub> produces highly reactive, short-living ·OH radicals. Generally, the resulting chemiluminescent emission is considerably higher than that from other mixtures.



At pH 8.5 the control chemiluminescence signal in this system reaches 17006 reference luminescent units (RLU) in the interaction between the reagents, the so-called fast flash, and usually decreases with time (Fig. 3A). The sample containing SiO<sub>2</sub> NPs follows this kinetics but with slightly lower values, representing the same levels and is not susceptible to oxidation by ROS. All other NMs

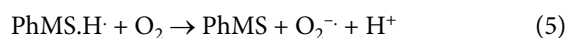
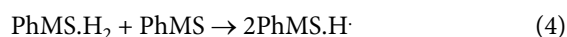
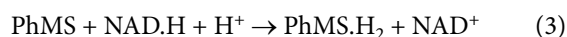
exhibit mild to strong prooxidant properties. ZnO NPs intensify the luminescent signal seven times, ZnO-SiO<sub>A</sub> almost three times, ZnO-SiO<sub>B</sub> more than two times, and most pronounced oxidation is registered with ZnO NCs 18 times. All kinetics is smooth, with no obvious peaks (Fig. 3A). At physiological pH 7.4 (Fig. 3B), almost the same effects are registered but at considerably lower levels; at this pH, ZnO-SiO<sub>A</sub> and ZnO-SiO<sub>B</sub> change places but maintain a mild prooxidant activity. Strong prooxidant activities exhibit the ZnO NCs almost four times and ZnO NPs and ZnO-SiO<sub>B</sub> NMs two times or less intensification of the signal.

#### • System II

In this system, hydrogen peroxide serves as both an oxidizing agent and a ROS. The results show that ZnO NCs are mostly oxidized at alkaline and neutral pH, respectively, and 30- and 5-times stronger signal than the controls. ZnO NPs exhibit almost 18 times (Fig. 3C) and about two times (Fig. 3D) stronger prooxidant activity compared to the control. At pH 8.5, ZnO-SiO<sub>B</sub> and ZnO-SiO<sub>A</sub> NPs expressed mild prooxidant effects, less than three times compared to the control signal (Fig. 3C). At pH 7.4, ZnO-SiO<sub>A</sub> provokes three times higher oxidation than ZnO-SiO<sub>B</sub> and the control (Fig. 3D). SiO<sub>2</sub> NPs demonstrate an extremely light prooxidant effect at both tested pH media.

#### • System III

The O<sub>2</sub><sup>·-</sup> generation in this system is believed to follow the chemical scheme of Nishikimi et al.<sup>30, 31</sup>



At alkaline tested conditions, ZnO NCs exhibit the strongest oxidation as their signal is 24 times higher than the control. ZnO NPs demonstrate almost two times stronger prooxidant activity than the control (Fig. 3E). The other tested synthesized NMs exhibit obvious antioxidant effects against the generated O<sub>2</sub><sup>·-</sup> radicals in the system 60 to 80% (Fig. 3E). The registered antioxidant activity is not

**Table 3.** Correlation coefficients between the sensitivity of chosen bacterial strains toward the antimicrobial effect of ZnO, ZnO NCs, ZnO-SiO<sub>A</sub>, and ZnO-SiO<sub>B</sub> NMs tested by spot diffusion and chemiluminescent assays.

Microorganism	System 1 pH 8.5	System 1 pH 7.4	System 2 pH 8.5	System 2 pH 7.4	System 3 pH 8.5	System 3 pH 7.4
<i>E. coli</i>	0.717	0.814	0.895	0.145	0.954	0.969
<i>BL21DE</i>						
<i>B. cereus</i>	0.921	0.970	0.996	0.496	0.998	0.814
<i>NBIMCC1095</i>						
<i>S. epidermidis</i>	0.797	0.879	0.943	0.266	0.984	0.932
<i>ATCC 12228</i>						



observed at pH 7.4 for all types of NPs. At physiological pH and provoked by the  $O_2^-$  radicals, ZnO NPs exhibit the strongest prooxidant activity compared to all tested systems and conditions (Fig. 3F). ZnO NCs show 16 times stronger signal than the control, followed by  $SiO_2$  (almost seven times), ZnO- $SiO_B$  (more than five times), and ZnO- $SiO_A$  (almost two times) (Fig. 3F). It should be noticed that in this ROS-generating system ( $O_2^-$ ),  $SiO_2$  presents a definitive prooxidant activity, which is not observed in the other tested systems.

Table 3 shows the correlation coefficients between the sensitivity of the chosen bacterial strains toward the antimicrobial effect of ZnO NPs, ZnO NCs, ZnO- $SiO_A$ , and ZnO- $SiO_B$  NPs tested by spot diffusion and chemiluminescent assays (1 mg/mL). Systems 1 and 3 show a strong correlation between the two assays. System 2 introduces a weak correlation in the case of *E. coli* and *S. epidermidis* and moderate correlation in the case of *B. cereus* at pH 7.4 despite the same system showing a strong correlation at pH 8.5. This confirms that the luminescent assay can be successfully applied at pH 8.5 for evaluating antimicrobial activity using System 2.

Nanosized ZnO's internalization and mechanistic activity depend on their physicochemical properties such as shape, size, charge, and surface.<sup>32</sup> Therefore, different shapes and sizes of ZnO NMs were synthesized by controlling the preparation conditions. Although the growth mechanism of NMs was extensively studied, the actual mechanism remains unknown. The general mechanism is believed to depend on solvent and growth conditions. Generally, alcohol group is extremely important in contributing the unoccupied oxygen to  $Zn^{2+}$  to form ZnO.<sup>33</sup> Then, small crystalline nuclei are formed by Ostwald ripening in a supersaturated reaction solution, followed by particle growth, and then large nanoparticles grow at the expense of small NPs.<sup>34</sup>

Moreover, by showing ZnO NCs' morphology in our experiment, Figure 1, these NMs look similar to agglomerates of small spheres. The growth mechanism of this form of ZnO NMs could be subject to the oriented attachment, a recent non-classical theory of crystal growth based on the repeated merging of adjacent particles on lattice-matched crystal facets; this is supported by TEM imaging (Figure 1B, inset).<sup>34</sup> Many research groups reported the preparation of ZnO aggregates;<sup>16</sup> however, the newly synthesized ZnO NCs in our experiment are well-packed clusters with high stability. XRD confirms the formation of hexagonal (wurtzite) structure of all synthesized ZnO NMs determined by the JCPDS card no. 01-080-3002, and no other phases were observed.

Based on our antibacterial test, it is clear that the  $SiO_2$  NPs and ZnO- $SiO_A$  were fully safe at concentrations up to 3 mg/mL, while all other investigated materials showed bactericidal effects at a higher concentration than 3 mg/mL. All tested bacterial *E. coli*, *Bacillus cereus*, and *S. epidermidis* showed high sensitivity toward ZnO NPs at 3

mg/mL. Both *E. coli* and *S. epidermidis* were inhibited at 1.5 mg/mL. Meanwhile, lower concentrations of ZnO NPs, however, were safe on all tested bacteria. It is worthy to notice that coating this nanomaterial with silica renders it completely safe for the bacteria at all concentrations. This could be attributed to the complete isolation of ZnO from the surrounding media by silica, which prevents Zn ions leakage from the particles, in addition to the safe action of silica on bacteria.<sup>35</sup> On the contrary, ZnO- $SiO_B$  shows higher toxicity compared to the naked silica particles. This could be attributed to the incomplete shielding of ZnO by silica in this case, which afforded a chance for ZnO leakage from these particles. Moreover, by referring to TEM images, ZnO- $SiO_B$  shows some aggregation that can increase the antibacterial action.<sup>28</sup> However, ZnO NCs demonstrated the strongest antibacterial effect if used in concentrations of 3 mg/mL and less. The mechanism that gives the advantage to ZnO NCs over ZnO NPs when the ZnO NC attaches to the cell membrane, it breaks down under the physiological conditions to its constituent of small spherical particles that duplicate and magnify the effect of ZnO NCs compared to one of the ZnO NPs. The most sensitive of all three tested bacteria were *Bacillus cereus* compared to *E. coli* and *S. epidermidis*, as shown in Table 2.

Our results are consistent with other studies that have reported the bactericidal effect of ZnO NMs. A few proposed mechanisms are the penetration of the NMs that release  $Zn^{2+}$ . Smaller NPs possibly penetrate cells, and hence they have a greater impact.  $Zn^{2+}$  would react with proteins, peptides, and amino acids, probably with phosphates and carbonates too, which will suppress many important cellular activities inside bacteria (active transport, metabolism, and enzyme activity), ultimately inducing the cell death.<sup>9</sup>

Others suggested that the antibacterial activity is not attributed to generated  $O_2^-$  rather than  $H_2O_2$ , with electrons and  $H^+$ .  $H_2O_2$  penetrates the membrane of bacteria, damaging its content such as proteins, lipids, and amino acids, causing cell death.<sup>12</sup> Moreover, we suggest that the outstanding antibacterial effect of ZnO NCs could be related to the random orientation of its cluster bars. We believe it is the same observation with the random-oriented ZnO nanoarrays (ROZN) outlined by Wang et al. who attributed the superior bactericidal effect of ROZN to cell membrane injury.<sup>36</sup>

Chemiluminescent assay results demonstrate the superiority of ZnO NCs over the rest of the tested NMs. One explanation could be that ZnO NCs are composed of small ZnO NPs, as shown in TEM images, which provide a slow release of ZnO for long periods, leading to a stronger effect on bacterial strains. In system I, the tested NPs are oxidized by the generated ROS in Fenton's system (Fig.3) that could explain the observed anti-inflammatory and antibacterial properties of those materials in the living systems. At physiological pH 7.4 (Fig.3B), almost the same effects are registered but at much lower levels because of the

change of pH of the media to a lower value. The achieved results from system II are confirmative on the stability of the tested newly synthesized NMs against  $H_2O_2$  as a typical strong oxidant, also generated in the living systems as part of their nonspecific inflammation reaction. In system III, ZnO NCs were susceptible to oxidation, followed by  $SiO_2$ , ZnO-SiO<sub>B</sub>, and ZnO-SiO<sub>A</sub>. Note that, in this ROS-generating system ( $O_2^-$ ),  $SiO_2$  presents a definitive prooxidant activity, unobserved in the other tested systems.

A detailed correlation analysis was performed of the sensitivity of the selected bacterial strains toward the antimicrobial effect of ZnO NPs, ZnO NCs, ZnO-SiO<sub>A</sub>, and ZnO-SiO<sub>B</sub> NPs, tested by the spot diffusion and chemiluminescent assays (1 mg/mL; Table 3). System I and III show a full positive correlation between the two assays. This is confirmative on the assumptions that  $\cdot OH$ ,  $\cdot OOH$ , and  $O_2^-$  radicals are part of the antimicrobial mechanism of the tested ZnO and its derived materials. System II introduces  $H_2O_2$  as a ROS and a strong oxidant. The correlation between system II and the spot-diffusion assay was moderate at pH 7.4; however, the correlation was strong at pH 8.5. This confirms that only reactions at pH 8.5 can be tested and followed to obtain reliable results on prooxidant, antimicrobial and bactericidal effects applying the chemiluminescent assay. The strength of the correlation coefficient follows the relationship level as perfect, strong, moderate, weak, and zero to the  $\pm$  values of 1.0, 0.7–0.9, 0.4–0.6, 0.1–0.3, and 0.<sup>37</sup> All achieved results are confirmative of the role of these ROS in the bactericidal effect in living systems. Although there are structural differences between Gram-positive and Gram-negative bacteria cell membranes, ZnO NMs show a strong effect on both types of bacteria, which depicts the broad spectrum of ZnO NMs effect.<sup>38</sup>

## 4. Conclusions

In this study, the different forms of newly synthesized ZnO NMs were prepared and tested against Gram-negative and Gram-positive bacteria. The agar diffusion test confirmed that ZnO NCs presented the best antimicrobial activity, while  $SiO_2$  and ZnO-SiO<sub>A</sub> NPs demonstrated no antibacterial activity. All NMs, except  $SiO_2$ , exhibit mild to strong prooxidant properties in the Fenton's system to generate ROS. ZnO NCs are a powerful oxidant. This could be explained by assuming that ZnO NCs are composed of small units of ZnO NPs that provide a slow release of ZnO for long periods, which leads to a stronger effect on bacterial strains.  $SiO_2$  is unsusceptible to oxidation by ROS.

The results achieved for both media demonstrate that all tested NMs are susceptible to oxidation by  $H_2O_2$ , a typical strong oxidant, also generated in the living systems as part of their nonspecific inflammation reaction. ZnO NCs and ZnO NPs exhibit strong oxidation in the alkaline tested conditions in system III. All other tested NMs ( $SiO_2$ ,

ZnO-SiO<sub>A</sub>, and ZnO-SiO<sub>B</sub>) exhibit pronounced 60%–80% antioxidant effects on the generated  $O_2^-$  radicals in the system. The registered antioxidant activity is not observed at pH 7.4 for any newly synthesized materials.

ZnO shows the strongest prooxidant activity compared to all the tested systems. The prooxidant effect is observed for all other materials too.  $SiO_2$  presents a definitive prooxidant activity, which is not observed in other systems. The correlation analysis on the sensitivity of the chosen bacterial strains toward the antimicrobial effect of ZnO NPs, ZnO-SiO<sub>A</sub>, and ZnO NCs tested using the spot-diffusion and chemiluminescent assays is highly confirmative on the role of these ROS ( $\cdot OH$ ,  $\cdot OOH$ ,  $H_2O_2$  and  $O_2^-$ ) in the bactericidal effect in living systems. Thus, ZnO NCs are an important antibacterial agent that could be an emergent replacement of traditional antibiotics.

## Funding

The Joint Research Project between The Institute of Biophysics and Biomedical Engineering, Bulgarian Academy of Sciences, Bulgaria and The Academy of Scientific Research and Technology (ASRT) and Nanotechnology and Advanced Materials Central Lab, Agricultural Research Centre, Egypt entitled “Biological activity of Nanocomposites materials with potential medical and microbiology application”. Project “Clean Technologies for Sustainable Environment – Waters, Waste, Energy for Circular Economy”, Ministry of Education and Science, Bulgaria, Contract Number: BG05M2OP001-1.002-0019.

## 5. References

1. B. Khameneh, R. Diab, K. Ghazvini and B. S. Fazly Bazzaz, *Microb. Pathog.* **2016**, *95*, 32–42. DOI:10.1016/j.micpath.2016.02.009
2. R. Y. Pelgrift and A. J. Friedman, *Adv. Drug Delivery Rev.* **2013**, *65*, 1803–1815. DOI:10.1016/j.addr.2013.07.011
3. N. Y. Lee, W. C. Ko and P. R. Hsueh, *Front. Pharmacol.* **2019**, *10*, 1–10.
4. G.-X. He and L.-W. Xue, *Acta Chim. Slov.* **2021**, *68*, 567–574. DOI:10.17344/acsi.2020.6333
5. L. Wang, C. Hu and L. Shao, *Int. J. Nanomed.* **2017**, *12*, 1227–1249. DOI:10.2147/IJN.S121956
6. A. Sirelkhatim, S. Mahmud, A. Seeni, N. H. M. Kaus, L. C. Ann, S. K. M. Bakhori, H. Hasan and D. Mohamad, *Nano-Micro Lett.* **2015**, *7*, 219–242. DOI:10.1007/s40820-015-0040-x
7. H. Y. Qian, *Acta Chim. Slov.* **2021**, *63*, 638–644. DOI:10.17344/acsi.2021.6656
8. SCCS (Scientific Committee on Consumer Safety), Addendum to the Opinion SCCS/1489/12 on Zinc oxide (nano form), **2014**, 1–13.
9. H. Mohd Yusof, R. Mohamad, U. H. Zaidan and N. A. Abdul Rahman, *J. Anim. Sci. Biotechnol.* **2019**, *10*, 57.

- DOI:10.1186/s40104-019-0368-z
10. J. Jiang, J. Pi and J. Cai, *Bioinorg. Chem. Appl.* **2018**, *2018*, 1062562–1062562. DOI:10.1155/2018/1062562
11. M. A. Ansari, H. M. Khan, A. A. Khan, A. Sultan and A. Azam, *Appl. Microbiol. Biotechnol.* **2012**, *94*, 467–477. DOI:10.1007/s00253-011-3733-1
12. L. Gabrielyan, A. Hovhannisyanyan, V. Gevorgyan, M. Ananyan and A. Trchounian, *Appl. Microbiol. Biotechnol.* **2019**, *103*, 2773–2782. DOI:10.1007/s00253-019-09653-x
13. L. Palanikumar, S. N. Ramasamy and C. Balachandran, *IET Nanobiotechnol.* **2014**, *8*, 111–117. DOI:10.1049/iet-nbt.2012.0008
14. D. Bartczak, M. O. Baradez, S. Merson, H. Goenaga-Infante and D. Marshall, *J. Phys.: Conf. Ser.* **2013**, *429*. DOI:10.1088/1742-6596/429/1/012015
15. F. Mohd Omar, H. Abdul Aziz and S. Stoll, *Sci. Total Environ.* **2014**, *468–469*, 195–201. DOI:10.1016/j.scitotenv.2013.08.044
16. K. Sahu, S. kuriakose, J. Singh, B. Satpati and S. Mohapatra, *J. Phys. Chem. Solids* **2018**, *121*, 186–195. DOI:10.1016/j.jpss.2018.04.023
17. E. G. Pantohan, R. T. Candidato, Jr. and R. M. Vequizo, *IOP Conf. Ser.: Mater. Sci. Eng.* **2015**, *79*, 6. DOI:10.1088/1757-899X/79/1/012024
18. R. K. Dutta, B. P. Nenavathu, M. K. Gangishetty and A. V. R. Reddy, *Colloids and Surfaces B: Biointerfaces* **2012**, *94*, 143–150. DOI:10.1016/j.colsurfb.2012.01.046
19. B. Abebe, E. A. Zereffa, A. Tadesse and H. C. A. Murthy, *Nanoscale Research Letters* **2020**, *15*, 190. DOI:10.1186/s11671-020-03418-6
20. E. L. Pavlova and V. M. Savov, *Biochemistry (Moscow)* **2006**, *71*, 861–863. DOI:10.1134/S0006297906080062
21. K. Faulkner and I. Fridovich, *Free Radical Biol. Med.* **1993**, *15*, 447–451. DOI:10.1016/0891-5849(93)90044-U
22. E. L. Pavlova, R. D. Toshkovska, T. E. Doncheva and I. A. Ivanova, *Arch. Microbiol.* **2020**, *202*, 1873–1880. DOI:10.1007/s00203-020-01902-2
23. G. Simonelli and E. L. Arancibia, *J. Mol. Liq.* **2015**, *211*, 742–746. DOI:10.1016/j.molliq.2015.07.075
24. H. A. Elshoky, E. Yotsova, M. A. Farghali, K. Y. Farroh, K. El-Sayed, H. E. Elzorkany, G. Rashkov, A. Dobrikova, P. Borisova, M. Stefanov, M. A. Ali and E. Apostolova, *Plant Physiol. Biochem.* **2021**, *167*, 607–618. DOI:10.1016/j.plaphy.2021.08.039
25. N. M. Shamhari, B. S. Wee, S. F. Chin and K. Y. Kok, *Acta Chim. Slov.* **2018**, *65*, 578–585. DOI:10.17344/acsi.2018.4213
26. D. Das, Y. Yang, J. S. O'Brien, D. Breznan, S. Nimesh, S. Bernatchez, M. Hill, A. Sayari, R. Vincent and P. Kumarathanan, *J. Nanomater.* **2014**, *2014*, 176015.
27. R. A. Howe, J. M. Andrews and f. t. B. W. P. o. S. Testing, *J. Antimicrob. Chemother.* **2012**, *67*, 2783–2784. DOI:10.1093/jac/dks391
28. A. Klančnik, S. Piskernik, B. Jeršek and S. S. Možina, *J. Microbiol. Methods* **2010**, *81*, 121–126. DOI:10.1016/j.mimet.2010.02.004
29. M. M. Tarpey, D. A. Wink and M. B. Grisham, *Am. J. Physiol. Regul. Integr. Comp. Physiol.* **2004**, *286*, R431–R444. DOI:10.1152/ajpregu.00361.2003
30. J. T. Hancock, R. Desikan and S. J. Neill, *Biochem. Soc. Trans.* **2001**, *29*, 345–349. DOI:10.1042/bst0290345
31. M. Nishikimi, N. Appaji Rao and K. Yagi, *Biochem. Biophys. Res. Commun.* **1972**, *46*, 849–854. DOI:10.1016/S0006-291X(72)80218-3
32. A. Happy, M. Soumya, S. Venkat Kumar and S. Rajeshkumar, *Chem.-Biol. Interact.* **2018**, *286*, 60–70. DOI:10.1016/j.cbi.2018.03.008
33. R. Razali, A. K. Zak, W. H. A. Majid and M. Darroudi, *Ceram. Int.* **2011**, *37*, 3657–3663. DOI:10.1016/j.ceramint.2011.06.026
34. D. Cao, S. Gong, X. Shu, D. Zhu and S. Liang, *Nanoscale Res. Lett.* **2019**, *14*, 210. DOI:10.1186/s11671-019-3038-3
35. F. Book, M. T. Ekvall, M. Persson, S. Lönnerud, T. Lammel, J. Sturve and T. Backhaus, *NanoImpact* **2019**, *13*, 100–111. DOI:10.1016/j.impact.2019.01.001
36. X. Wang, F. Yang, W. Yang and X. Yang, *Chem. Commun.* **2007**, 4419–4421. DOI:10.1039/b708662h
37. H. Akoglu, *Turkish J. Emerg. Med.* **2018**, *18*, 91–93. DOI:10.1016/j.tjem.2018.08.001
38. A. Ali, S. Ambreen, R. Javed, S. Tabassum, I. ul Haq and M. Zia, *Mater. Sci. Eng. C* **2017**, *74*, 137–145. DOI:10.1016/j.msec.2017.01.004

## Povzetek

Nanomateriali na osnovi cinkovega oksida (ZnO) nudijo nekaj obetavnih protibakterijskih učinkov. V okviru te študije je bila sintetizirana nova oblika ZnO, imenovana »ZnO palčke nanogrozdov« (angl. ZnO nanocluster bars, NC). Pripravljeni in okarakterizirani so bili ZnO NC, nanodelci ZnO (NP), ZnO, prevlečen s silicijevim dioksidom (ZnO-SiO<sub>A</sub>, ZnO-SiO<sub>B</sub>) in SiO<sub>2</sub> nanodelci, pri čemer je bila testirana tudi njihova protimikrobna in prooksidantna aktivnost. Prooksidantno aktivnost vseh nanomaterialov je bila preučevana glede na reakcije oksidacije s prostimi radikali (pH 7,4 in pH 8,5) v kemiluminiscentnih modelnih sistemih. Vsaka oblika na novo sintetiziranih nanomaterialov ZnO je pokazala edinstveno obnašanje, ki je v Fentonovem sistemu zajemalo vse od blagih do močnih prooksidativnih lastnosti. ZnO NP in ZnO NCs so pokazali močne protibakterijske učinke, ZnO-SiO<sub>A</sub> NPs pa niso pokazali nobene protibakterijske aktivnosti, ki bi predstavljala biokompatibilnost. Vse testirane NM so bile tudi podvržene oksidaciji s H<sub>2</sub>O<sub>2</sub>. Pri ZnO NC in ZnO NPs se je zgodila močna oksidacija v O<sub>2</sub><sup>-</sup> generatorskem sistemu pri pH 8,5. Medtem ko so SiO<sub>2</sub>, ZnO-SiO<sub>A</sub> and ZnO-SiO<sub>B</sub> izkazovali izrazite 60–80 % antioksidativne učinke, so SiO<sub>2</sub> NP delovali kot dokončni prooksidant, česar v drugih testih niso opazili. ZnO NC so močno oksidirani, ob predpostavki, da ZnO NC zagotavljajo počasnejše sproščanje ZnO, kar vodi v močnejši učinek na bakterijske seve. ZnO NC so torej pomembno protibakterijsko sredstvo, ki bi lahko nadomeščalo tradicionalne antibiotike.



Except when otherwise noted, articles in this journal are published under the terms and conditions of the Creative Commons Attribution 4.0 International License